Chemical Abundances in Gaseous Nebulae
AAA Workshop Series 10, 2016
G. Hägele, M. Cardaci & E. Pérez-Montero, eds.

Invited Review

Metal content in the central region of galaxies

M.V. Cardaci[1,2], G.F. Hägele[1,2], A.I. Díaz[3], P. Rodríguez-Pascual[4], M. Santos-Lleó[4] and O.L. Dors[5]

[1]*Instituto de Astrofísica de La Plata (CONICET-UNLP), Argentina*
[2]*Facultad de Ciencias Astronómicas y Geofísicas, Universidad Nacional de La Plata, Paseo del Bosque s/n, 1900 La Plata, Argentina*
[3]*Facultad de Ciencias, Universidad Autónoma de Madrid, C/Francisco Tomás y Valiente 7, Ciudad Universitaria de Cantoblanco, 28049 Madrid, Spain.*
[4]*XMM-Newton Science Operations Center, ESAC, ESA, POB 78, 28691 Villanueva de la Cañada, Madrid, Spain*
[5]*Universidade do Vale do Paraíba, Av. Shishima Hifumi, 2911, Cep12244-000, Saõ José dos Campos, SP, Brazil*

Abstract. Accurate abundance determinations for the central regions of a great amount of galaxies would be necessary to improve the calibration of abundances in the over solar regime. Circumnuclear Star Forming Regions (CNSFRs) in early type galaxies, being close to the galactic nuclei, are expected to be of high metal content and in fact empirical abundance indicators constructed with strong optical emission lines point to oversolar abundances up to 3 times solar. Due to the difficulty in deriving abundances directly the calibrations have to be provided by theoretical photoionization models which require several assumptions to be made. Different models/assumptions provide different calibrations. The optical observational analysis of the warm ionized gas of CNSFRs yields oxygen abundances lower than expected from empirical abundance indicators. These findings point to a deficiency of light alpha elements (O, Ne) in the central regions of M 82. If this is common among regions dominated by recent star formation, the estimated oxygen abundances might not be representative of the true metal content of these regions. This could have a profound effect on abundance calibrations leading to fundamental relations like the Mass-Metallicity and Luminosity-Metallicity relations. X-ray emission analysis can provide abundances for the hot gas phase. This hot plasma is thought to be mainly heated by the supernovae explosions so that the X-ray gas should trace the current abundances of the galaxies. These alternative estimations of the metal content of the central region of galaxies would provide new observational constrains for models of chemical evolution.

1. Introduction

Metallicity studies are intended to disentangle the chemical evolution of the Universe. Stars convert H into heavier elements that enrich their environments as the stars evolve and die. Being the third most abundant element (after H and He) the oxygen is a good metallicity tracer in the interstellar medium. HII regions, planetary nebulae, and supernova remnants usually display prominent emission lines of oxygen.
Metallicities of galaxies have been mainly derived by measuring nebular optical emission-lines associated with their giant HII regions. More used elements to determine metallicities in HII regions are oxygen and neon. In spiral galaxies negative gradients with higher abundances towards the galactic centers were found (e.g. Vílchez et al., 1988; Vila-Costas & Edmunds, 1992; Sánchez et al., 2014).
The method applied on each region depends on the intensity of the diagnostic lines. The direct method (Te-method) consist in the determination of O and N abundances through the electron temperature (Te). The major diagnostic Te line is the weak auroral [OIII]λ4363Å emission-line. In high metallicity environments the cooling carried on by some elements makes this [OIII]λ4363Å line, no longer observable. In these cases semi-empirical strong-lines methods were proposed to derive abundances. Semi-empirical methods are based on model assumptions for the geometry and nature of the ionizing source, and the determination of a large number of correlated physical parameters (e.g. U, Teff, Z) that have to be calibrated through the comparison between some strong-line ratios predicted by the models with the ones estimated from observational data. Depending on the adopted calibrations quite different abundances are able to reproduce the observed strong-lines ratios.
Díaz et al. (1989) reported metallicity estimations through the CaII and MgI near-IR lines. They conclude that in the low metallicity regime the strength of the CaII triplet is only a function of the metal abundance and hence it is a useful metallicity indicator in such metal poor systems. These absorption lines are produced by the stars in the HII region, hence they provide a way to estimate stellar abundances. Stellar metallicities trace the galactic enrichment at the time of the stars birth i.e. prior to the last burst of star formation, while hot gas metallicities trace the enrichment produced by the ongoing burst as elements are carried to the interstellar medium (ISM) by stellar winds and supernova explosions.
Star forming regions also emit in X-rays. A recent star formation event is characterized by the presence of diffuse X-ray emission associated with the hot gas, and compact sources associated with massive X-ray binaries and supernova remnants (e.g. Fabbiano, 1989). The interaction of supernovae with the ionized shells formed by winds from massive stars is an efficient producer of X-ray emission in star-forming regions (Chu & Mac Low, 1990; Shull & Saken, 1995; Tenorio-Tagle et al., 2006). This hot plasma is thought to be mainly heated by the supernovae explosions so that the X-ray gas should trace the current abundances of the galaxies. Therefore, the analysis of the X-ray emission would provide abundances for the hot gas phase.

2. Why the central region of galaxies?

The inner parts of some near barred spiral galaxies, as for example NGC 3351 and NGC 3310, show intense star-forming regions frequently arranged in a roughly anular pattern of about 1 kpc in diameter around their nuclei. This regions are called Circumnuclear Star Forming Regions (CNSFRs). These star forming complexes have sizes ranging between a few tens to a few hundreds of pcs (see e.g. Díaz & Pérez-Montero, 2000) and seem to be made up of several HII regions ionized by luminous compact stellar clusters of only a few pc in size, as measured from high spatial resolution HST images (Hägele et al., 2007, 2009, 2010b; Hägele, 2008).

In general, the circumnuclear HII regions are similar to the giant HII regions found in the disks of galaxies, although the circumnuclears are more compact and present a higher peak surface brightness Kennicutt et al. (1989) than their disks counterparts. Their large Hα luminosities, typically higher than 10^{39} erg s^{-1} point to relatively massive star clusters as their ionization source (10^5 - 10^6 $M_\odot$), which minimizes the uncertainties due to small number statistics when applying population synthesis techniques (see e.g. Cerviño et al., 2002). The present of multiple components in their emission-line profiles showing different kinematical behaviours (Hägele et al., 2007, 2009, 2010b) regards important doubts about the properties of the ionized gas derived from global emission-line measurements (Hägele et al., 2013). The lack of detection at radio wavelengths in the central region of NGC 3351 could imply that the ionizing population of their CNSFRs are too young (less than a few Myr) to host supernovae (Hägele et al., 2010a).

Being close to the galactic nuclei, CNSFRs are expected to be of high metal abundance and, in fact, empirical abundance indicators constructed with strong emission lines, point to oversolar abundances up to three times solar. Therefore these regions are very interesting labs since the star-formation is taking place in a high metallicity environment and could provide clues for the understanding of star formation phenomena at large metallicities and, due to its position in the galaxies, for the determination of metallicity gradients in spiral galaxies. For example, for NGC 3310, the abundances of the CNSFR were derived by Pastoriza et al. (1993) from direct measurements of the electron temperature and were found to be under solar while the nucleus showed twice solar abundances.

A dozen of these structures in three other galaxies (NGC 3351, NGC 2903 and NGC 3504) have been studied by Hägele during his PhD Thesis Hägele (2008) and by Díaz et al. (2007). These authors estimated the abundances were found using a new semi-empirical method including emission lines from the far blue to the far red (3600 to 10000 Å). Some of the relevant results that these authors found are that the oxygen abundances of these regions are consistent with solar values; only one of the analyzed CNSFRs shows a metallicity higher than solar (by a factor of 1.5); their ionization structure, as mapped by the [OII]/[OIII] ratios as a function of the [SII]/[SIII] ratios point to relatively hard ionizing sources, contrary to what is expected in high metallicity environments. Hence, no three times oversolar abundances as predicted by abundance empirical indicators were found. A similar result was found later by Sánchez et al. (2014) in 26 over the 193 galaxies ($\sim$ 13.5%) of the sample selected for the CALIFA project.

Regarding the X-ray emission as metallicity tracer of the hot ISM gas, no much was done but in a handful of objects (e.g. N 253, Ptak et al. 1997; NGC 1569,

Martin et al. 2002; NGC 1365, Pagel et al. 1979). The most detailed abundance derivations from emission line analyses of hot gas in this band has been done for the starburst galaxy M 82 using XMM-Newton data.
Read & Stevens (2002) modelled the XMM-Newton high resolution spectra (RGS) using MEKAL models (Mewe et al., 1995) with a sixth order Chebyshev polynomial. They found near solar abundances of O and Fe, and oversolar abundances of Mg ($X/X_{\odot} \sim 2.3$-5.2), Si($X/X_{\odot}>4.6$) and Ne($X/X_{\odot}>1.4$). Relative OVII(r,f,i) intensities are consistent with collisionnally ionized gas in equilibrium.
Origlia et al. (2004) compared stellar-abundances from near-IR absorption spectra with hot gas abundances from X-rays spectra of M 82. They found a solar abundance of O and half solar of Fe from the stellar component; and half hot gas phase metallicities than the ones reported by Read & Stevens (2002) with the same XMM-Newton observation (RGS+EPIC). It is noteworthy that these authors found different solar abundances of the elements than those found by Read & Stevens, but similar abundance ratios between these elements than them. The low O abundance found by Origlia and collaborators ($X/X_{\odot} \sim 0.3$) is difficult to explain in the framework of the α-element enhancement by SN II explosions.
Ranalli et al. (2008) analysed (in a comprehensive way) a long X-rays observation (110 ks) of M 82. They also compared two of the more often used X-rays models to characterize the hot plasma: MEKAL (Mewe et al., 1995) and APEC (Smith et al., 2001). They found that part of the Optical-to-Xrays difference found by Origlia et al. in the O abundance could be attributed to the charge-exchange emission. This effect was not taken into account previously and is produced when the hot wind encounters with cold neutral gas, ions from the wind diffuse through the interface into the cold gas where electrons are transferred from neutrals to ions. Both the resulting ions can be highly excited and re-arrange their electrons by emitting photons in the extreme UV and the X-ray bands. From the comparison between MEKAL and APEC X-rays models Ranalli and collaborators concluded that there is still needed a fine-tuning between them since they provided different abundances of the elements, but similar abundance ratios between them. These authors also found that the O and N abundances in M 82 are lower/equal to the solar ones.
The detailed abundance study performed in the X-ray band for M 82 has provided unexpected results. In the inner ~ 1 kpc of the galaxy both the hot gas and the stars trace a very similar Fe abundance. Nevertheless, while the ratios of the heavier α-elements (Mg, S) over Fe are enhanced in the hot gas, the lighter α-elements (O, Ne) are not; in fact, they are depressed. If this behavior is common in the central regions of galaxies, the oxygen abundances derived from the ionized gas might not be representative of the true metal content of these regions.

3. Discussion

The fact that the optical analysis of the warm ionized gas in CNSFRs yields an oxygen abundance lower than expected from empirical abundance indicators points to an effect similar to what found in M 82, that is a deficiency of light α-elements (O, Ne) in these central regions.
Our aim is to analyze the X-ray emission of the central zone hosting circumnuclear ring of the two spiral galaxies: NGC 3310 and NGC 2903 for which we have

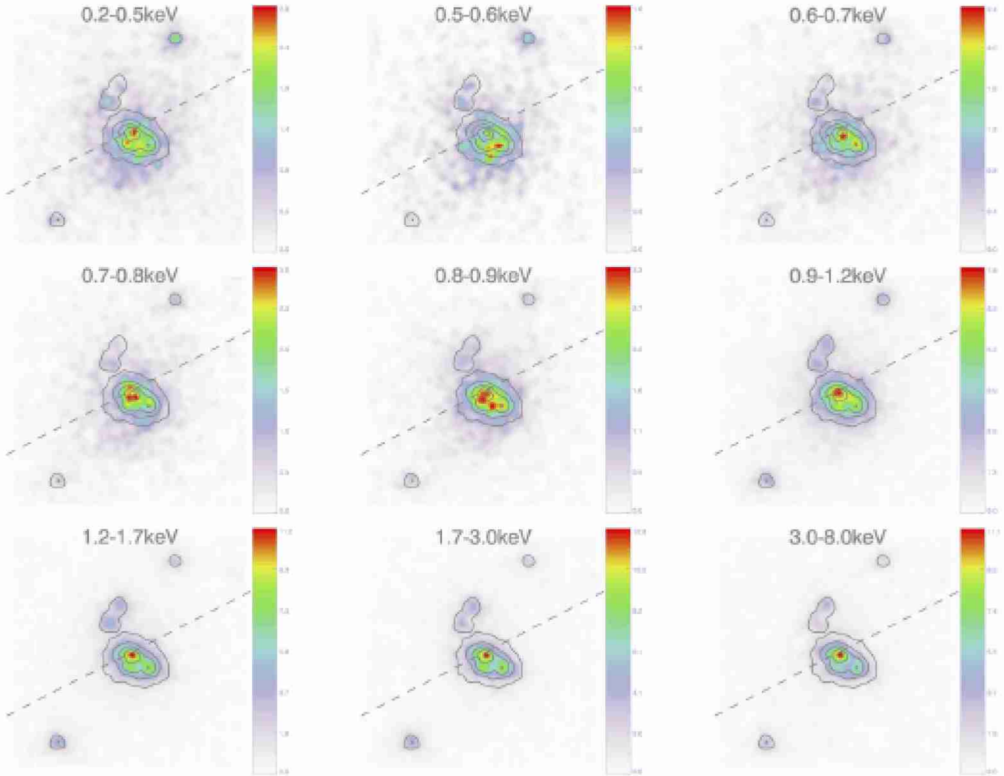

Figure 1. EPIC-MOS images in nine energy intervals selected to compare the distribution of the X-rays from the softness to the hardness ranges.

derived abundances (Pastoriza et al., 1993; Díaz et al., 2007) and gas and star kinematical information as much as estimations of the dynamical masses of the CNSFRs and the ionizing clusters (Hägele et al., 2009, 2010b), and for which X-ray emission has already been detected.

At the objects distances (~8-15 Mpc) the integrated RGS spectra would encompass the central galaxy region with the circumnuclear ring. This is suitable for us since all the CNSFRs in a given galaxy show comparable (optical) abundances and we are interested in the average abundance of the hot gas associated with the collection of individual star-forming structures.

A previous XMM-Newton observation of NGC 3310, of about 11 ks of effective exposure time, shows hints for the presence of emission lines giving the appropriate scientific case to achieve time for a longer observation. NGC 3310 was re-observed using the XMM-Newton satellite on 2008-2009. The allocated 110 ks observation was performed in two runs of about 55 ks each with an year between them. After the first run, the signal-to-noise improvement was already significant. Comparing the first short observation with data of our first run it shows up clearly that the signal-to-noise improvement is significant.

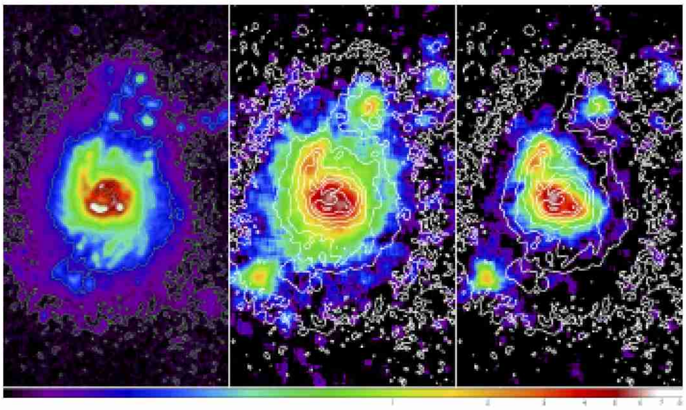

Figure 2. Right: UV image acquired during the first run of our observation using the OM camera on-board the XMM-Newton satellite (UVW1 filter with $\lambda_{\rm eff} = 2910$Å). Middle: soft X-rays EPIC camera data with the UV contours over-plotted. Right: hard X-rays EPIC camera data with the UV contours over-plotted.

Using the lower resolution EPIC data cubes acquired simultaneously with the RGS spectra we were able to analyze the morphology of the observed field as a function of the energy. In Fig. 1 we can see that in the soft X-ray band the emission is extended and that the emitting zone turns out more compact as the radiation turns harder. Comparing the morphology of the central region of this galaxy in UV, soft and hard X-rays we see that, in general, the X-rays spatial distribution follows the UV emission, in spite of there are strong X-rays emitters that have not an UV counterpart (see Fig. 2).
NGC3310 has also been observed using the ACIS-S camera on board the Chandra satellite. This camera has a spatial resolution of 1 arcsec and a moderate spectral resolution similar to the EPIC-MOS cameras on board the XMM-Newton satellite. The high spatial resolution of the Chandra satellite allows the identification of punctual sources and broad spectral features, but ACIS-S spectral resolution is not enough to identify narrow features in the soft band as the ones needed to perform an abundance study. Comparing contours from our XMM-Newton EPIC-pn camera data (with a spatial resolution of 6 arcsec) with Chandra data we can see a perfect match in the identification of the emitting regions (see, Fig. 3).
Once the whole observation ($\sim$ 110 ks) was performed, we have combined the RGSs data from both data set cleaning high background periods and correcting for effective exposure times. Fig. 4 shows the RGS data displayed as being a long slit. In this figure we see well identified high excitation emission lines (e.g. NeIX, FeXVII and OVIII). As the gas physical properties in X-rays are derived performing model fitting, the more significant lines we have, the more accurate model parameter values we can obtain.

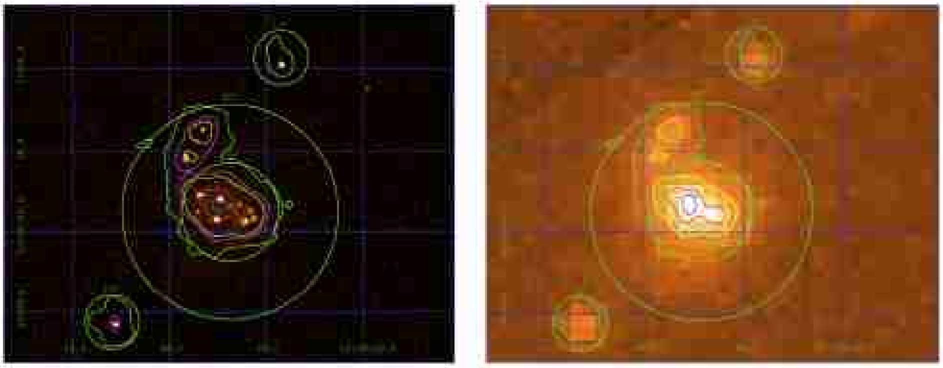

Figure 3. XMM-Newton EPIC-pn contours over-plotted on the Chandra ACIS-S image (left) and the EPIC-pn image (right).

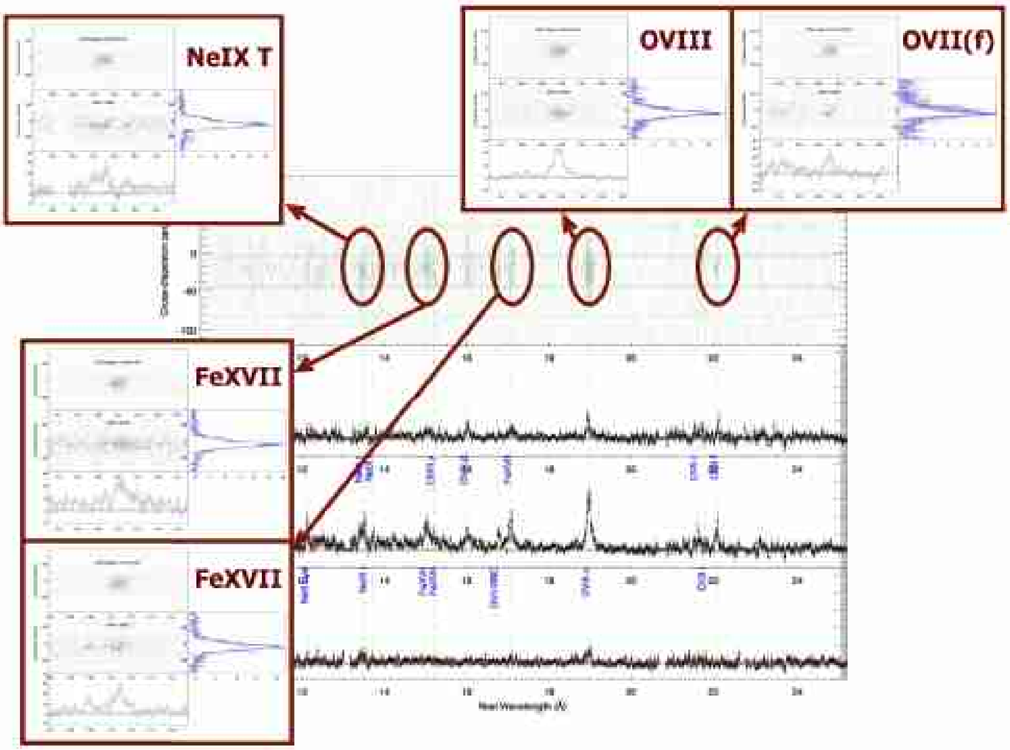

Figure 4 Combined RGSs data from the two runs cleaned for high background periods and corrected by effective exposure times displayed as RGSs be long slit spectrographs. Most prominent features are identify and for each one we obtained spatial profiles. In the remarked boxes RGS and EPIC spatial distribution for these features are compared.

4. Summary

The central regions of some spiral galaxies have metallicities lower than predicted by abundance empirical indicators. This is also the case for a group of spirals hosting Circumnuclear Star Forming Regions. From optical data it has been found that these regions, located at about 1 kpc from the nucleus, show about solar abundances, what makes them good places to study with the aim of disentangling the enrichment process.

It is possible to obtain metallicities using data in the X-rays band to compare it with the ones obtained in other bands. The method is still new and needs to be fine tuned. Our aim is to perform the metallicity study using very good X-rays data of NGC 3310 and NGC 2903. In our RGS spectra significant high excitation lines are clearly identified. The relative intensities between the components of the Ne IX $\lambda\lambda$13.4, 13.6, 13.7 Å and O VII $\lambda\lambda$21.6, 21.8, 22.1 Å triplets are sensitive to the temperature and density of the plasma (e.g. Porquet & Dubau, 2000), hence they could be used to characterize the media where they are formed.

Acknowledgments. The scientific work reported in this article involves observations obtained with XMM-Newton, an ESA science mission with instruments and contributions directly funded by ESA Member States and NASA. The scientific work reported in this article made use of data obtained from the Chandra Data Archive.

References

Cerviño M., Valls-Gabaud D., Luridiana V., et al., 2002, *A&A*, **381**, 51
Chu Y.-H., Mac Low M.-M., 1990, *ApJ*, **365**, 510
Díaz A. I., Pérez-Montero E., 2000, *MNRAS*, **312**, 130
Díaz A. I., Terlevich E., Castellanos M., et al., 2007, *MNRAS*, **382**, 251
Díaz A. I., Terlevich E., Terlevich R., 1989, *MNRAS*, **239**, 325
Fabbiano G., 1989, *ARA&A*, **27**, 87
Hägele G. F., 2008, *Ph.D. thesis*, Universidad Autónoma de Madrid
Hägele G. F., Ascasibar Y., Richards A. M. S., et al., 2010a, *MNRAS*, **406**, 1675
Hägele G. F., Díaz A. I., Cardaci M. V., et al., 2007, *MNRAS*, **378**, 163
Hägele G. F., Díaz A. I., Cardaci M. V., et al., 2009, *MNRAS*, **396**, 2295
Hägele G. F., Díaz A. I., Cardaci M. V., et al., 2010b, *MNRAS*, **402**, 1005
Hägele G. F., Díaz A. I., Terlevich R., et al., 2013, *MNRAS*, **432**, 810
Kennicutt Jr. R. C., Keel W. C., Blaha C. A., 1989, *AJ*, **97**, 1022
Martin C. L., Kobulnicky H. A., Heckman T. M., 2002, *ApJ*, **574**, 663
Mewe R., Kaastra J. S., Liedahl D. A., 1995, *Legacy*, **6**, 16
Origlia L., Ranalli P., Comastri A., Maiolino R., 2004, *ApJ*, **606**, 862
Pagel B. E. J., Edmunds M. G., Blackwell D. E., et al., 1979, *MNRAS*, **189**, 95
Pastoriza M. G., Dottori H. A., Terlevich E., et al., 1993, *MNRAS*, **260**, 177
Porquet D., Dubau J., 2000, *A&AS*, **143**, 495
Ptak A., Serlemitsos P., Yaqoob T., et al., 1997, *AJ*, **113**, 1286
Ranalli P., Comastri A., Origlia L., Maiolino R., 2008, *MNRAS*, **386**, 1464
Read A. M., Stevens I. R., 2002, *MNRAS*, **335**, L36
Sánchez S. F., Rosales-Ortega F. F., Iglesias-Páramo J., et al., 2014, *A&A*, **563**, A49

Shull J. M., Saken J. M., 1995, *ApJ*, **444**, 663
Smith R. K., Brickhouse N. S., Liedahl D. A., Raymond J. C., 2001, *ApJL*, **556**, L91
Tenorio-Tagle G., Muñoz-Tuñón C., Pérez E., Silich S., Telles E., 2006, *ApJ*, **643**, 186
Vila-Costas M. B., Edmunds M. G., 1992, *MNRAS*, **259**, 121
Vílchez J. M., Pagel B. E. J., Díaz A. I., Terlevich E., Edmunds M. G., 1988, *MNRAS*, **235**, 633